LETTERS
PUBLISHED ONLINE: 6 MAY 2011 | DOI: 10.1038/NCLIMATE1086
nature climate change

Interdecadal modulation of El Niño amplitude during the past millennium

Jinbao Li[1,2]*, Shang-Ping Xie[1,3,4], Edward R. Cook[2], Gang Huang[5], Rosanne D'Arrigo[2], Fei Liu[1], Jian Ma[3] and Xiao-Tong Zheng[4]

The El Niño/Southern Oscillation (ENSO) is the dominant mode of interannual climate variability on Earth, alternating between anomalously warm (El Niño) and cold (La Niña) conditions in the tropical Pacific at intervals of 2–8 years[1,2]. The amplitude of ENSO variability affects the occurrence and predictability of climate extremes around the world[3,4], but our ability to detect and predict changes in ENSO amplitude is limited by the fact that the instrumental record is too short to characterize its natural variability[5–8]. Here we use the North American Drought Atlas[9,10]—a database of drought reconstructions based on tree-ring records—to produce a continuous, annually resolved record of ENSO variability over the past 1,100 years. Our record is in broad agreement with independent, ENSO-sensitive proxy records in the Pacific and surrounding regions. Together, these records indicate that ENSO amplitude exhibits a quasi-regular cycle of 50–90 years that is closely coupled to the tropical Pacific mean state. Anomalously warm conditions in the eastern Pacific are associated with enhanced ENSO variability, consistent with model simulations[11]. The quasi-periodic ENSO amplitude modulation reported here offers a key observational constraint for improving models and their prediction of ENSO behaviour linked to global warming.

Despite great efforts to understand the El Niño/Southern Oscillation (ENSO) phenomenon, there is still much uncertainty in changes in ENSO amplitude. Instrumental records indicate marked variations in ENSO amplitude, large around the 1890s–1900s and 1970s–1990s, but small between these periods and before 1890 (Supplementary Fig. S1). Existing proxy records suggest significant variability in ENSO amplitude in the past[2,12,13], but they cover only the past few centuries or noncontinuous periods of the past millennium. Current general circulation models (GCMs) give different projections of future ENSO-related change, with some showing an increase and others no change or even a decrease in ENSO amplitude[6,7]. Therefore, it is crucial to develop long, continuous, high-resolution proxy records to determine the characteristics of natural ENSO variability, and to provide observational constraints for improving the models[7,8].

Proxy records from the equatorial Pacific are valuable for studying past ENSO behaviour[12–14], yet very few such records exist. This situation has impeded the study of long-term ENSO amplitude modulation. By contrast, thousands of tree-ring records without these deficiencies are available for North America, a region where hydroclimate is sensitive to tropical Pacific climate anomalies on various timescales[15,16]. Such tree-ring records have been used to develop the gridded North America Drought Atlas[9,10] (NADA) (see Methods and Supplementary Information). Here we demonstrate the fidelity of NADA in recording long-term ENSO variability, particularly variations in ENSO amplitude on interdecadal to centennial timescales.

The leading empirical orthogonal function (EOF) of NADA, which accounts for 23.5% of the total variance, shows a distinct moisture pattern heavily loaded over southwest North America (Methods and Fig. 1a), a region strongly affected by ENSO variability[15,16]. The explained variance of the first EOF for the southwest North America domain rises to 49.5% (Supplementary Fig. S3), and its principal component (PC) has a correlation of 0.99 with that for the whole of North America over the past 1,100 years. This confirms that NADA PC1 dominates variability in southwest North America.

The fidelity of NADA PC1 in representing ENSO variability is demonstrated in five ways: (1) NADA PC1 is significantly correlated with equatorial Pacific sea surface temperatures[17] (SSTs) during the instrumental period (Fig. 1c). For example, its correlation with the January–March (JFM) ENSO Niño3 index for 1870–2002 is 0.51 ($P < 0.001$) (Supplementary Fig. S4). (2) NADA PC1 is significantly correlated with a modern coral record from Palmyra Island in the central tropical Pacific[13], at $r = -0.58$ for the common period 1891–1994 ($P < 0.001$) (Supplementary Fig. S5). After adjusting relict coral U/Th dates within the analytical error windows[13], we found possible correlations between North American drought and tropical corals that persisted throughout the past millennium (Methods and Fig. 1d). Considering the independent nature of these proxy records, this agreement is remarkable, strongly indicative of a coherent relationship between ENSO and North American drought over the past millennium. (3) NADA PC1 is highly correlated with, but is significantly longer than, the existing ENSO reconstructions (Supplementary Table S1). Most of these reconstructions are largely, although not entirely, independent, as they only share a few common tree-ring data from southwest North America. This suggests that NADA PC1 represents reasonable estimates of ENSO variability over the past millennium. (4) Separate composite analysis of NADA for periods of large and small PC variability over the past millennium shows nearly identical patterns (Supplementary Fig. S6). This pattern stability suggests that the westerly waveguide is stable in tropical forced stationary waves, and that NADA PC1 represents the modulation of ENSO itself. (5) Separate EOF analysis shows that the first EOF of NADA is heavily loaded over southwest North America both before and after the 1976/1977 climate regime shift[18,19], and the PC is highly correlated with tropical eastern Pacific SSTs for both periods

[1]International Pacific Research Center, University of Hawaii at Manoa, Honolulu, Hawaii 96815, USA, [2]Lamont-Doherty Earth Observatory, Columbia University, Palisades, New York 10964, USA, [3]Department of Meteorology, University of Hawaii at Manoa, Honolulu, Hawaii 96815, USA, [4]Physical Oceanography Laboratory and Ocean–Atmosphere Interaction and Climate Laboratory, Ocean University of China, Qingdao 266100, China, [5]Institute of Atmospheric Physics, Chinese Academy of Sciences, Beijing 100029, China. *e-mail: jinbao@hawaii.edu.

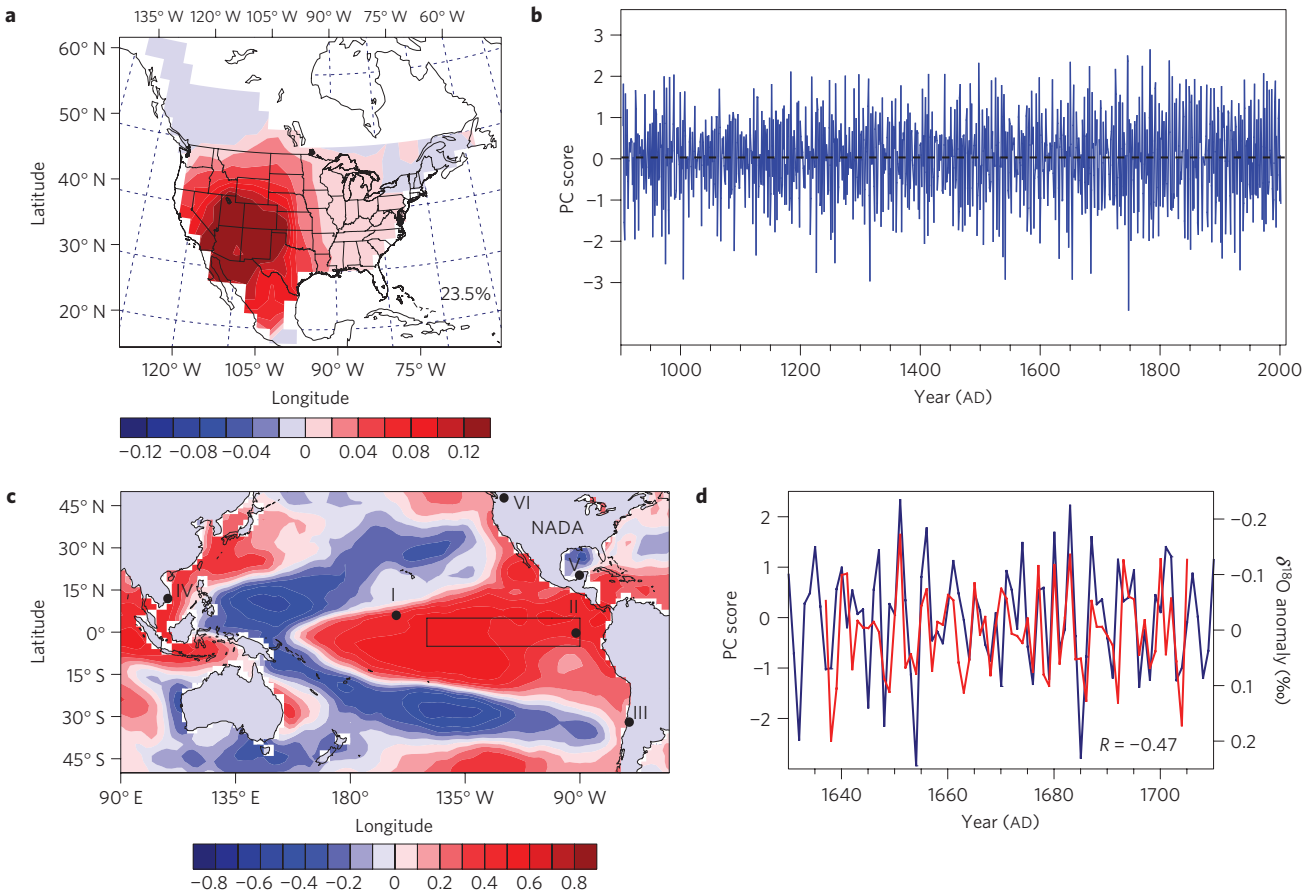

Figure 1 | The leading EOF pattern of NADA, its PC series and correlation of the PC series with tropical records. a, Spatial pattern of the leading EOF over North America, and **b**, its PC time series. The percentage variance accounted for by the leading EOF is labelled in **a**. **c**, Spatial correlation of NADA PC1 with global JFM SSTs (ref. 17) during 1870–2002. The SSTs were processed using a 9-yr Lanczos high-pass filter[30] to isolate interannual variability. The box denotes the Niño3 region, and the dots indicate the site locations mentioned in the text (I: Palmyra corals[13], II: Galápagos coral[12], III: Chile tree rings[23], IV: Vietnam tree rings[24], V: Mexico sediment[26], VI: Washington sediment[27]). **d**, Comparison of NADA PC1 (blue) with the dating-error corrected Palmyra relict coral δ^{18}O series[13] (red) over 1637–1705.

(Supplementary Fig. S7). Although there exist some differences in the EOF pattern and correlation with tropical SSTs between the two periods, these results indicate that moisture variability in southwest North America has been sensitive to ENSO variability both before and after the 1976/1977 climate regime shift. The relationship to ENSO is further confirmed by the SST correlation pattern for 1870–2002 (Fig. 1c). Therefore, teleconnections of canonical eastern Pacific ENSO (hereafter simply ENSO) are probably stable over southwest North America. On the basis of these validations, we consider that NADA PC1 represents a continuous record of interannual ENSO variability during the past millennium.

As inferred from NADA PC1, ENSO amplitude has been highly variable during the past millennium, with many El Niño/La Niña events of larger amplitude than observed in the instrumental period (Fig. 1b). Here we calculated a 21-yr running biweight variance[20] to measure changes in ENSO amplitude. This technique highlights the interdecadal amplitude modulation of a time series while reducing bias that might be introduced by extreme outliers in a 21-yr window. As shown in Fig. 2a, superimposed on a general rising trend are large fluctuations in ENSO variance on interdecadal to centennial timescales. ENSO variance was reduced in the Medieval Climate Anomaly (MCA) period, with the eleventh-century variance being the lowest of the past millennium. Following this, the variance showed an increasing trend in the Little Ice Age (LIA), and maintained a high level from the eighteenth century to the Current Warm Period (CWP). On average, the eighteenth-century ENSO variance was the strongest of the past millennium.

A multi-taper method[21] (MTM) spectral analysis reveals two significant quasi-regular periodicities at 50–60-yr and 82–90-yr bands, respectively (Fig. 3a), confirming the visual impression of interdecadal modulation of ENSO amplitude. A time-space wavelet transform[22] exhibits a marked shift in the dominant periodicity, concomitant with the transition from the MCA into the LIA, from a 82–90-yr cycle during AD 900–1300 to a 50–60-yr cycle thereafter (Fig. 3b). Meanwhile, a 30-yr cycle is present during AD 1500–1800 and in the MTM analysis. The shifts in ENSO periodicity, together with a general increase in variance (Fig. 2a), may reflect major reorganizations within the tropical ocean–atmosphere system, or alternatively significant ENSO teleconnection changes from the MCA to LIA.

We found evidence for such interdecadal fluctuations in ENSO variance elsewhere, especially in the equatorial Pacific and regions under strong ENSO teleconnections. Variance modulation in North American tree rings is consistent with that observed in the Niño3 SST, and the two variance series are correlated at 0.64 ($P < 0.001$) during their common period 1880–1992 (Fig. 2a). A coral annual average oxygen isotopic (δ^{18}O) record from the Galápagos Islands in the eastern equatorial Pacific[12] exhibits quasi-periodic variance modulation similar to that in North American tree rings during the past four centuries (Fig. 2b). The coral δ^{18}O records from Palmyra Island in the central tropical Pacific[13], although not continuous,

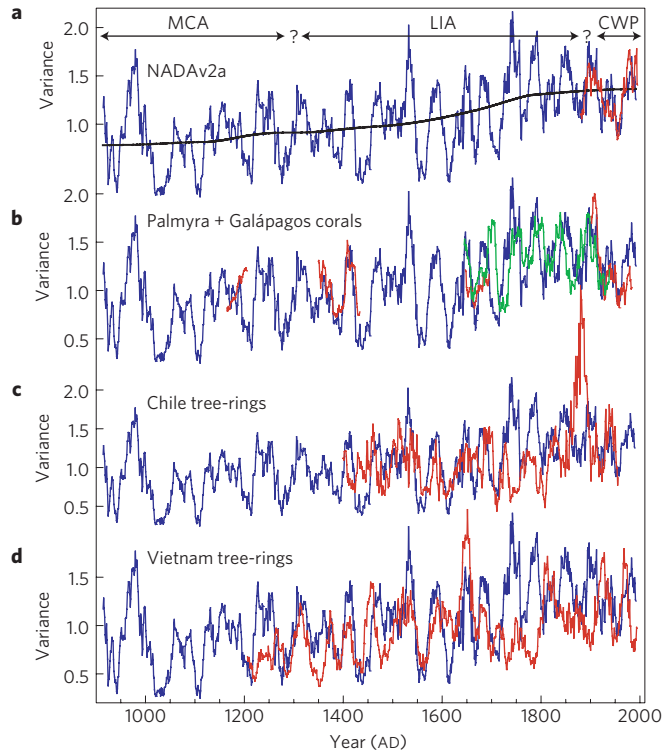

Figure 2 | Comparison of records of ENSO variance. NADA-derived ENSO variance (blue) along with those derived from: **a**, the observed Niño3 SST (ref. 17; red) over 1880–1995; **b**, coral records from both the Galápagos Islands in the eastern equatorial Pacific[12] (green) and Palmyra Island in the central tropical Pacific[13] (red); **c**, tree-ring record from an ENSO-sensitive site in El Asiento, Chile[23] (red); **d**, tree-ring record from the Bidoup Nui Ba National Park in southern Vietnam[24] (red). All records were processed using a 9-yr Lanczos high-pass filter[30] before calculating a 21-yr running biweight variance. The black bold line in **a** denotes a 400-year low-pass filter to indicate the long-term trend.

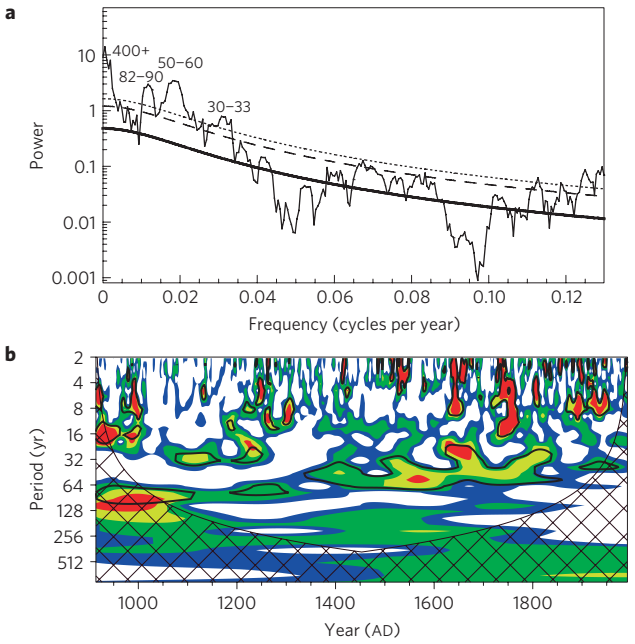

Figure 3 | Spectral property of the NADA-derived ENSO variance series. **a**, MTM (ref. 21) spectral density of the ENSO variance series. The bold line indicates the null hypothesis, and the dash (dotted) line indicates the 95% (99%) significance level, using a red-noise background spectrum. Periodicities of significant peaks are labelled above the spectral density line. **b**, The wavelet power spectrum[22]. The power has been scaled by the global wavelet spectrum. The cross-hatched region is the cone of influence, where zero padding has reduced the variance. Black contour is the 90% significance level, using a red-noise background spectrum.

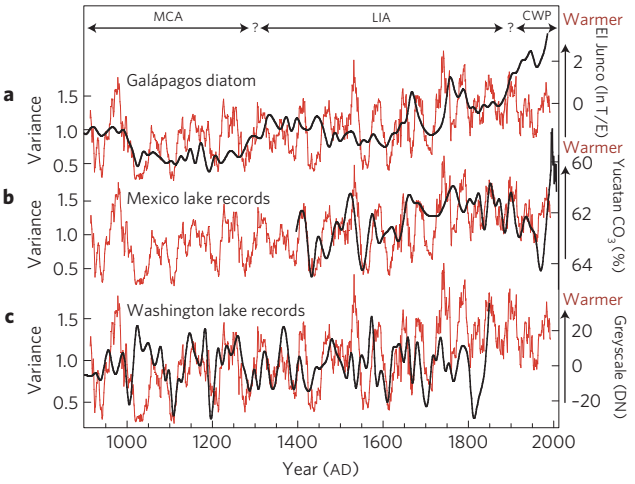

Figure 4 | Comparison of the NADA-derived ENSO variance series with records of the tropical Pacific mean state. NADA-derived ENSO variance (red) along with: **a**, a diatom record from El Junco Lake, Galápagos, in the eastern equatorial Pacific[14] (black). **b**, A carbonate ion (CO_3^{2-}) record from Aguada X'caamal Lake in northwest Yucatan, Mexico[26] (black). **c**, A greyscale record from Castor Lake in Washington state, USA (ref. 27) (black). All lake records were smoothed using a 9-yr low-pass filter. Upward swings in black curves represent a warm state of the tropical Pacific.

show broadly consistent changes in variance during the past nine centuries (Fig. 2b). Tree-ring records from an ENSO-sensitive site in El Asiento, Chile, in the Southern Hemisphere[23], exhibit similar interdecadal fluctuations in variance over most of the past six centuries, except during the late nineteenth century, when there is an out-of-phase relationship (Fig. 2c). Recent tree-ring records from the highlands of Bidoup Nui Ba National Park in southern Vietnam[24], a tropical region strongly influenced by ENSO teleconnections, also show in-phase fluctuations in variance with North American tree-rings during the thirteenth to seventeenth and most of the twentieth centuries, although this relationship was out-of-phase during the eighteenth to nineteenth centuries (Fig. 2d). We note two caveats of the above proxy comparisons. First, unlike the NADA, which is based on nearly two-thousand tree-ring chronologies across North America, other proxy data often consist of only a single series for a given site, and are prone to chaotic noise and regional variability. Second, the long-term stability of ENSO influence in other teleconnection regions needs further investigation, unlike North America where we have validated a persistent relationship to ENSO during the past millennium. Overall these records from the tropics and mid-latitudes in both the Northern and Southern Hemispheres are mutually consistent. Together they show quasi-periodic amplitude modulation, and suggest that such modulation is fundamental to ENSO physics.

How ENSO amplitude modulation is related to changes in the tropical Pacific mean state is a key question for ENSO physics[6,11,25]. Here we examine this relationship during the past millennium by comparing the NADA-derived ENSO variance series with three proxy records for the tropical Pacific mean state. The first is a diatom record from El Junco Lake, Galápagos, an indicator of SSTs in the eastern equatorial Pacific[14] (Fig. 4a). The second is a carbonate ion (CO_3^{2-}) record from Aguada X'caamal Lake in

northwest Yucatan, Mexico (Fig. 4b) that indicates SST changes in the surrounding ocean[26]. The third is a greyscale record from a sediment core from Castor Lake in the Pacific Northwest, whose low-frequency variations are interpreted as changes in the tropical and extratropical Pacific mean state[27] (Fig. 4c).

Despite discrepancies that may reflect either data uncertainties or changes in SST spatial structure, these three records indicate that the eastern tropical Pacific was in a cooler state at the peak of the MCA (~AD 1000–1200), and that there was a persistent positive temperature trend in the LIA and CWP (Fig. 4). ENSO variance was thus greatly reduced during most of the MCA, increased persistently in the LIA, and maintained a high level in the CWP. Moreover, interdecadal fluctuations in ENSO variance seem closely related to anomalies in the Pacific mean state during the past millennium. The Castor Lake data, in particular, suggest that a warm (cool) eastern tropical Pacific is associated with increased (reduced) ENSO variance over most of the 1,000-year record (Fig. 4c). These observations suggest that ENSO variability during the past millennium is closely coupled to changes in the background mean state, a finding that is supported by recent model simulations[6,11].

The quasi-regular nature of ENSO amplitude modulation, and the co-variations with the equatorial Pacific mean state, support the emerging idea that there is a positive feedback between the mean state and ENSO variance[11]. An increase in ENSO amplitude causes the eastern equatorial Pacific to warm, a mean-state change that amplifies ENSO variability. If fully tested in observations and process-oriented model studies, this idea can be exploited for decadal prediction of ENSO amplitude.

In summary, using data on North American tree rings, we have produced a continuous, annually resolved record of ENSO variability for the past millennium. This record is in broad agreement with independent proxy records in and surrounding the Pacific over most of their common periods, revealing a marked quasi-regular interdecadal modulation of ENSO amplitude throughout the past millennium. The amplitude modulation is closely associated with changes in the tropical Pacific mean state, suggesting an interactive relationship. This observation alone implies that the continued increase in eastern-central tropical Pacific SSTs in a future warmer climate[5,7] will lead to enhanced ENSO variability and more extreme climate conditions around the globe. The diverse response of a host of ocean–atmospheric feedbacks complicates such a prediction of ENSO amplitude change[5,7]. Regardless, the quasi-periodic modulation of ENSO amplitude provides a crucial observational constraint that can be used to guide model improvement towards reduced uncertainties in predicting future ENSO behaviour. Finally, the further study of the mechanisms responsible for such ENSO amplitude modulation (for example, stochastic atmospheric noise[28] and external forcing[29]) will help shed light on ENSO dynamics.

Methods

The updated North America Drought Atlas (NADA). The NADA (ref. 9) consists of annually resolved summer (June–August) Palmer Drought Severity Index (PDSI) reconstructions derived from tree rings, available on a 2.5° × 2.5° grid over most of North America (Supplementary Information). Compared with the initial release of the NADA, the updated version (NADAv2a) used more tree-ring chronologies (1845 in total) to improve the PDSI reconstructions, but the grid spacing, series length, and statistical methods remain unchanged[10]. Here we analyse the updated NADA for AD 900–2006, a period when reconstructed values are available at more than 60% of all grid points (Supplementary Fig. S2). Time series at each grid point were processed using a 9-yr Lanczos high-pass filter[30] to preserve variability in the classical ENSO band of 2–8 years[1,2]. Empirical orthogonal function (EOF) analysis was used to objectively define the dominant mode of summer drought over NA, and the associated principal component (PC) series was used to indicate its variability over time.

Relict coral dating error corrections. By splicing together relict coral oxygen isotopic (δ^{18}O) records from Palmyra Island in the central tropical Pacific, Cobb *et al.*[13] provided 30-150-yr windows of tropical Pacific climate variability over the past 1,100 years. Their modern coral samples were exactly dated, whereas relict corals were dated using the U/Th method, which contains a general dating error of ± 5–10-yr. Therefore, if there were a coherent relationship between ENSO and North American drought over the past millennium, then, by adjusting the relict coral sequences within the range of their U/Th-dating errors, a firm match could be achieved between the coral δ^{18}O sequences and NADA PC1.

We first examined the modern coral record. As NADA PC1 represents seasonally averaged moisture variability that has its highest correlation with winter (January–March) tropical Pacific SSTs, we herein used the January–March mean coral δ^{18}O records to make them directly comparable. All series were processed using a 9-yr Lanczos high-pass filter[30] to highlight interannual variability. The highest correlation of the modern coral δ^{18}O record with NADA PC1 over their common period 1891–1994 is −0.58, which is close to its correlation with the Niño3 index (−0.61) in the same period. The highest correlation was achieved at lag zero, confirming that there is no dating error for modern coral. This good match between modern coral and NADA PC1 corroborates the dating error correction method.

The seventeenth-century sequence was spliced from three relict coral δ^{18}O records (SB3, SB13, and SB8), and was correlated at −0.06 with NADA PC1 before dating errors were corrected. Dating error for each of the three individual series was corrected by adjusting years within the range of U/Th-dating errors. A firm match with NADA PC1 was achieved for each series after dating adjustments, with correlations improved from 0.17 to −0.41 for SB3, −0.20 to −0.62 for SB13, and −0.27 to −0.51 for SB8. After correcting the dating errors and re-splicing the three sequences together, a good match between relict corals and NADA PC1 was achieved, with a correlation of −0.47 over their common period 1637–1705 (Supplementary Fig. S4). Similarly, dating errors were corrected for the fourteenth–fifteenth-century sequence, and its correlation with NADA PC1 improved from −0.14 to −0.35 over the common period 1339–1443.

The tenth- and twelfth-century sequences are both single relict coral δ^{18}O records. The best match between the tenth-century sequence and NADA PC1 was achieved after adjusting the start year of the relict coral sequence from AD 933 to AD 931, and their correlation over the common period 931–954 improved from 0.08 to −0.43. The correlation of the twelfth-century sequence with NADA PC1 over their common period 1154–1215 is −0.19, and there is no significant improvement when its dating was adjusted within the range of its U/Th-dating error. Therefore, we did not make a dating error correction for this sequence.

Received 21 December 2010; accepted 25 March 2011; published online 6 May 2011

References

1. Deser, C., Alexander, M. A., Xie, S-P. & Phillips, A. S. Sea surface temperature variability: Patterns and mechanisms. *Annu. Rev. Mar. Sci.* **2,** 115–143 (2010).
2. D'Arrigo, R., Cook, E. R., Wilson, R. J., Allan, R. & Mann, M. E. On the variability of ENSO over the past six centuries. *Geophys. Res. Lett.* **32,** L03711 (2005).
3. McPhaden, M. J., Zebiak, S. E. & Glantz, M. H. ENSO as an integrating concept in Earth science. *Science* **314,** 1740–1745 (2006).
4. Tang, Y., Deng, Z., Zhou, X., Cheng, Y. & Chen, D. Interdecadal variation of ENSO predictability in multiple models. *J. Clim.* **21,** 4811–4833 (2008).
5. Collins, M. *et al.* The impact of global warming on the tropical Pacific Ocean and El Niño. *Nature Geosci.* **3,** 391–397 (2010).
6. Yeh, S. W. & Kirtman, B. P. ENSO amplitude changes due to climate change projections in different coupled models. *J. Clim.* **20,** 203–217 (2007).
7. Guilyardi, E. *et al.* Understanding El Niño in ocean–atmosphere general circulation Models: Progress and challenges. *Bull. Am. Meteorol. Soc.* **90,** 325–340 (2009).
8. Wittenberg, A. T. Are historical records sufficient to constrain ENSO simulations? *Geophys. Res. Lett.* **36,** L12702 (2009).
9. Cook, E. R., Woodhouse, C., Eakin, C. M., Meko, D. M. & Stahle, D. W. Long-term aridity changes in the western United States. *Science* **306,** 1015–1018 (2004).
10. Cook, E. R. *et al. North American Summer PDSI Reconstructions, Version 2a.* IGBP PAGES/World Data Center for Paleoclimatology Data Contribution Series # 2008-046 (NOAA, NGDC Paleoclimatology Program, 2008).
11. Choi, J., An, S-I., DeWitte, B. & Hsieh, W.W. Interactive feedback between the tropical Pacific Decadal Oscillation and ENSO in a coupled general circulation model. *J. Clim.* **22,** 6597–6611 (2009).
12. Dunbar, R. B., Wellington, G. M., Colgan, M. W. & Glymn, P. W. Eastern Pacific sea surface temperature since 1600 AD: The δ^{18}O record of climate variability in Galápagos coral. *Paleoceanography* **9,** 291–315 (1994).
13. Cobb, K. M., Charles, C. D., Cheng, H. & Edwards, R. L. El Niño/Southern Oscillation and tropical Pacific climate during the last millennium. *Nature* **424,** 271–276 (2003).
14. Conroy, J. L. *et al.* Unprecedented recent warming of surface temperatures in the eastern tropical Pacific Ocean. *Nature Geosci.* **2,** 46–50 (2009).
15. Seager, R., Kushnir, Y., Herweijer, C., Naik, N. & Velez, J. Modelling of tropical forcing of persistent droughts and pluvials over western North America: 1856–2000. *J. Clim.* **18,** 4068–4091 (2005).

16. Cook, E. R., Seager, R., Cane, M. A. & Stahle, D. W. North American droughts: Reconstructions, causes and consequences. *Earth Sci. Rev.* **81,** 93–134 (2007).
17. Smith, T. M., Reynolds, R. W., Peterson, T. C. & Lawrimore, J. Improvements to NOAA's historical merged land–ocean surface temperature analysis (1880–2006). *J. Clim.* **21,** 2283–2296 (2008).
18. Mantua, N. J., Hare, S. R., Zhang, Y., Wallace, J. M. & Francis, R. C. A Pacific interdecadal climate oscillation with impacts on salmon production. *Bull. Am. Meteorol. Soc.* **78,** 1069–1079 (1997).
19. Zhang, Y., Wallace, J. & Battisti, D. ENSO-like decade-to-century scale variability: 1900–93. *J. Clim.* **10,** 1004–1020 (1997).
20. Lanzante, J. R. Resistant, robust & non-parametric techniques for the analysis of climate data: Theory and examples, including applications to historical radiosonde station data. *Int. J. Climatol.* **16,** 1197–1226 (1996).
21. Mann, M. E. & Lees, J. Robust estimation of background noise and signal detection in climatic time series. *Clim. Change* **33,** 409–445 (1996).
22. Torrence, C. & Compo, G. P. A practical guide to wavelet analysis. *Bull. Am. Meteorol. Soc.* **79,** 61–78 (1998).
23. LaMarche, V. C. Jr., Holmes, R. L., Dunwiddie, P. W. & Drew, L. G. Tree-ring chronologies of the southern hemisphere: Chile. *Lab. Tree-Ring Res. Chronol. Ser.* **2,** 1–43 (1979).
24. Buckley, B. M. *et al*. Climate as a contributing factor in the demise of Angkor, Cambodia. *Proc. Natl Acad. Sci. USA* **107,** 6748–6752 (2010).
25. Fedorov, A. V. & Philander, S. G. A stability analysis of the tropical ocean–atmosphere interactions: Bridging measurements and theory for El Niño. *J. Clim.* **14,** 3086–3101 (2001).
26. Hodell, D. A. *et al*. Climate change on the Yucatan Peninsula during the Little Ice Age. *Quat. Res.* **63,** 109–121 (2005).
27. Nelson, D. B. *et al*. Drought variability in the Pacific Northwest from a 6,000-yr lake sediment record. *Proc. Natl Acad. Sci. USA* doi:10.1073/pnas.1009194108 (2011).
28. Burgman, R. J., Schopf, P. & Kirtman, B. P. Decadal modulation of ENSO in a hybrid coupled model. *J. Clim.* **21,** 5482–5500 (2008).
29. Mann, M. E., Cane, M. A., Zebiak, S. E. & Clement, A. Volcanic and solar forcing of the tropical Pacific over the past 1,000 years. *J. Clim.* **18,** 447–456 (2005).
30. Duchon, C. E. Lanczos filtering in one and two dimensions. *J. Appl. Meteorol.* **18,** 1016–1022 (1979).

Acknowledgements

We gratefully acknowledge the researchers who have contributed their tree-ring data for NADA development. This research was funded by the National Science Foundation, the National Oceanic and Atmospheric Administration, the Japan Agency for Marine-Earth Science and Technology, the National Basic Research Program of China (2011CB309704), and the National Science Foundation of China (No.40890155). This is a International Pacific Research Center/School of Ocean and Earth Science and Technology Contribution (774/8128) and a Lamont–Doherty Earth Observatory Contribution (7462).

Author contributions

J.L., S-P.X. and E.R.C. contributed to data analysis. J.L., S-P.X., E.R.C., G.H., and R.D. contributed to writing the paper. All authors discussed the results and commented on the manuscript.

Additional information

The authors declare no competing financial interests. Supplementary information accompanies this paper on www.nature.com/natureclimatechange. Reprints and permissions information is available online at http://npg.nature.com/reprintsandpermissions. Correspondence and requests for materials should be addressed to J.L.